Asian Journal of Convergence in Technology *Volume III, Issue III*
ISSN No.:2350-1146, I.F-2.71

Investigation on Three-Dimensional CFD Validation for a Variable Span Morphing Wing

Musavir Bashir and Parvathy Rajendran*
School of Aerospace Engineering,
Universiti Sains Malaysia
14300 Nibong Tebal, Malaysia
aeparvathy@usm.my

Akshay Mule
Department of Aerospace Engineering
Indian Institute of Aeronautical Engineering & Information Technology, Pune, Maharashtra, India.

***Abstract*— This paper presents the computational design validation of a morphing wing profile that allows a change in the wing aspect ratio. Generally, the aerodynamic performance can be enhanced by changing the aspect ratio of the wing. Variable span morphing wing allows two distinct airfoil sections of the wing to extend its span using another section employing strap driven mechanism. The primary airfoil model section is maintained by NACA 4412 with span of 1.05 meters with full extension to 1.50 meters. Therefore, both two dimensional and three dimensional computational studies are carried out in a span morphed wing and un-morphed wing for various angles of attack respectively. It is found that the extended wing gives better aerodynamic performance and improved range. However, the separation phenomenon and turbulence occurs in the transition regions of wing profile. CFD FLUENT are used to understand the different flow patterns and pressure variations over the various sections of the wing. This study also demonstrates the potential effectiveness of a model meshing on the simulation and emphasizes the sensitivity of the solution outcome to the model solution setup.**

Keywords*— *Aerodynamic Performance; Wing Design; Span Morphing; Computational Fluid Dynamics.

I. INTRODUCTION

Changing operating conditions and multi-mission requirements, aerospace vehicles are engaged in a number of phases. Therefore, it is beneficial to optimize the aircraft to meet all these multi-mission maneuvers. Usually the optimization can be achieved by completing mission using fixed geometrical configuration. But this results in the design compromise by affecting the efficiency of other operating phases.

For example, an aircraft designed for loiter at low speed, where high speed dashes are preformed between loiter way-points, might favor a design that maximizes the aspect ratio for the loiter condition, constrained by the requirements of the high speed dash, such as engine thrust, or power, or wing loading [1]. This may lead to lower potential dash speed or shorter range and/or endurance.

As a result, the adaptive wing is like an avian flight that has capability to adjust its wings to meet multiple flight maneuvers with better performance. Morphing aircraft bestows the unique ability to increase the efficiency as compared to conventional aircrafts.

Various morphing aircraft designs are being investigated by engineers. Approaches of wing morphing include span change [2], wing twist [3], wing sweep change [4], and wing camber [5]. A variable span configuration has ability to meet the requirements of both military and commercial UAVs. Increasing the wingspan, increases the aspect ratio and wing area, and decreases the span-wise lift distribution for the same lift.

Thus, the drag of the wing could be decreased, and consequently, the range or endurance of the vehicle increase. The applications of smart materials with their morphing outcomes have also been summarized, and different mechanisms have been listed to achieve multi-mission aerospace vehicles [6].

II. CURRENT RESEARCH AND DESIGNS

Span morphing technology offers a strategy to modify the wing aspect ratio, and the wing planform to optimize the flight conditions. One such study was presented by employing span morphing on the mission performance of a 25-kg UAV [7]. The analyses were performed in order to increase the aerodynamic efficiency or range.

Models that were undertaken are adaptive aspect ratio (AdAR) span morphing. The results indicate that generally morphing for span morphing, the aerodynamic efficiency is maximized for a 30%–70% to 40%–60% weighting between the low and high speed flight conditions. Maximizing the effect of span morphing is dependent on the operational speed range, in addition to the weighting of the mission between low and high speed.

Other design model into investigation was Gear driven autonomous twin spar (GNATSpar) [8]. The GNATSpar can be used to achieve span extensions up to 100% but for demonstration purposes it is used here to achieve span extensions up to 20% to reduce induced drag and increase flight endurance. The span extension increased the

aerodynamic efficiency of the UAV. The GNATSpar requires relatively large force required to morph the wing with the flexible skin.

The Zigzag wing-box concept was studied and it allowed the wing span to be varied by 44% (22% extension and 22% retraction) [9]. The Zigzag wing-box consists of a rigid part and a morphing part. The rigid part is a semi-monocoque construction that houses the fuel tank and transfers the aerodynamic loads from the morphing part to the fuselage.

Also, known as the Adaptive Aspect Ratio wing, this concept couples a compliant skin to a mechanism based internal structure to create a morphing wing capable of significant changes in span and aspect ratio as shown in Fig. 1.

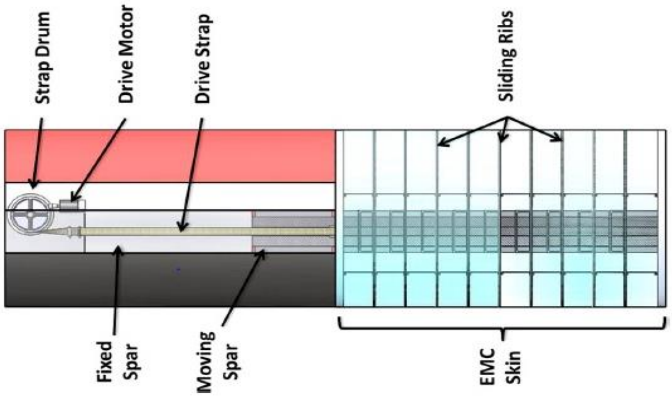

Fig 1. Adaptive aspect ratio wing [10]

Therefore, the current study aims to provide a research overview in determining the research simulation validation of a variable span wing. The computational validation has been performed to determine the efficacy of morphing.

III. Numerical Strategy and Optimization

To verify the aerodynamic coefficients, the numerical analysis performed is compared to the earlier results found in the literature. The wing area and the aspect ratio of a conventional wing are fixed. For lift augmentation, the lift coefficient can be increased by enlarging the angle of attack of the wing profile.

However, in adaptive wings, same can be achieved by increasing the aspect ratio via changing the area of the wing. The parameters of total drag (C_D), profile drag (C_{Do}) and induced drag (C_{Di}) is defined and related aspect ratio to enhance the aerodynamic efficiency as follows [11].

$$R = \frac{\eta}{C_f}\frac{C_L}{C_D}\ln\left(\frac{W_0}{W_1}\right) \tag{1}$$

$$E = \frac{\eta}{C_f}\frac{C_L^{3/2}}{C_D}\sqrt{2\rho_\infty S}\left(\frac{1}{\sqrt{W_1}}-\frac{1}{\sqrt{W_0}}\right) \tag{2}$$

$$\left(\frac{C_L}{C_D}\right)_{\max} = \frac{\left(C_{Do}\pi eAR\right)^{1/2}}{2C_{Do}} \tag{3}$$

$$\left(\frac{C_L^{3/2}}{C_D}\right)_{\max} = \frac{\left(3C_{Do}\pi eAR\right)^{3/4}}{4C_{Do}} \tag{4}$$

It is noted that both range and endurance are strongly dependent on $\frac{C_L}{C_D}$ and $\frac{C_L^{3/2}}{C_D}$ respectively. Each of these ratios is dependent on the wing aspect ratio. Thus, it is clear that an increase in wing aspect ratio would result in an increase in both range and endurance.

In addition, endurance is further enhanced for a variable aspect ratio wing because wing surface area also increases with aspect ratio. By tailoring the wing geometry one can adapt the lift and drag characteristics to a variety of missions.

A. Model Development

A three dimensional geometric model was developed using CAD design modeler software as in Fig. 2. In order to facilitate the solution, the geometric model should be small and simple in design, but must meet all the requirements of each individual part with maximum accuracy.

Fig. 2. CAD wing Model

The smaller model provides checked meshing nodes, and the mesh grid quantity will directly impact the solution duration. It is noted that the model of the wing is NACA4412 profile with chord of 0.5 m and full span of 1.5 m respectively. The extended model observed will be employed after validating the solution for the NACA airfoil.

B. Model Meshing

After the three-dimensional wing model is created using CAD design software, it is imported to GAMBIT for mesh generation. The model meshing is the most significant and refined process in CFD simulations. The characteristics of meshing are determined by the technique of the meshing.

Innumerous grid cells or elements are created in the meshing process which is required to solve all the desired fluid flow equations. The grid size has a significant impact on the computational time which in turn influences the cost of

simulations. The grid will also have a significant effect on the convergence speed and solution accuracy.

In case of successful computations of turbulent flows in a wing model, some boundary layer considerations are also required in mesh generation. Due to strong interaction of the mean flow and turbulence, the numerical results of the turbulent flow show more sensitivity towards the grid dependency than laminar flow.

The grouping of the grid in the direction normal to the surface solves the boundary layer solution, with the spacing of the first grid point off the wall to be well within the laminar sub-layer of the boundary layer.

Therefore, hexagonal or prism elements are employed to discrete boundary layers to preserve the accuracy in the wall normal direction for highly stretched viscous grid. The meshing models of both the un-extended and extended wing profiles can be seen in Fig. 3 and 4 respectively.

Aerodynamic coefficients being the focus of investigations in an aerodynamic wing, the surface gridding strategy with defined element size should be taken based on the local chord length. A size of 0.1% of local chord length at leading and trailing edge is good enough to resolve the flow physics and about 5% of the local chord length is good enough to resolve the flow phenomenon along the span-wise direction.

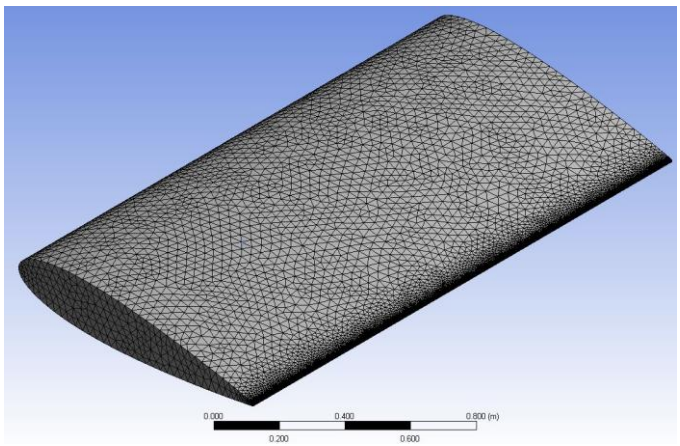

Fig. 3. Surface Mesh over the un-extended Wing profile

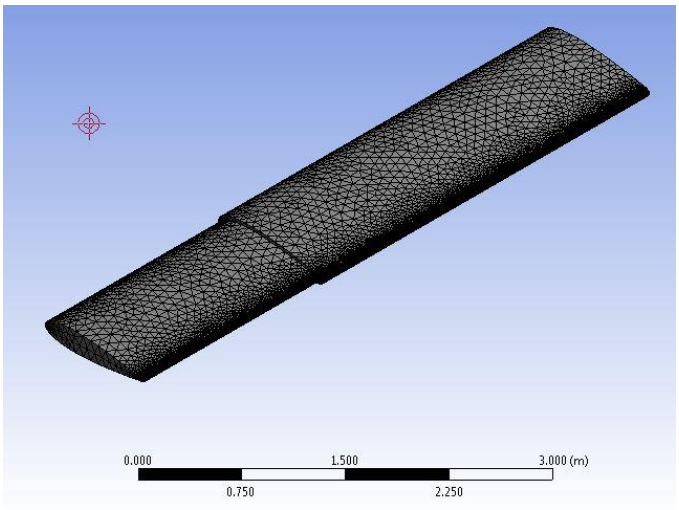

Fig. 4. Surface Mesh over the extended wing profile

Furthermore, the condition of viscous flow is significant and the boundary layer resolution also plays a greater role in determining the Cd values. Y+ is the governing factor for boundary layer meshing. In order to avoid the different wall functions in simulation, the values of Y+ factor must be less than 1.

Introducing the course meshing and proceeding towards the fine meshing, Y+ values can be 1, 0.67, 0.44 and 0.3. Also, the growth rate of elements should be less than 1.25 to obtain an optimum solution.

C. Model Solution Set-Up

After importing the geometry in to ANSYS®/GAMBIT, the mesh is generated and 3D solution domain is set. In order to obtain the optimum solution, two distinct rectangular prisms are created, termed as inner domain and outer domain.

The inner domain is much smaller than the outer domain but it comprises ten times more elements than that of the outer domain. The inner domain is nested in such a way that the pressure gradients are higher in the surface of the wing than the far zones. The selection of this small growth size enables dense mesh density in the inner solution domain which is presented in Fig. 5.

Pave type Tri elements are used on wing surface. The inner volume between the wing and inner rectangular prism is meshed by using T Grid type Tet/Hybrid elements. The growth rate for the elements is 1.09 from the wing surfaces to the inner rectangular prism surfaces. The element concentration is denser over wing surfaces as shown in Fig. 6.

This enables a better solution for the pressure gradient on the wing surfaces. Leading and trailing edge of the wing is important from the pressure gradient point of view. Around the edges, the element size is smaller than the element size on the middle section of the wing surfaces.

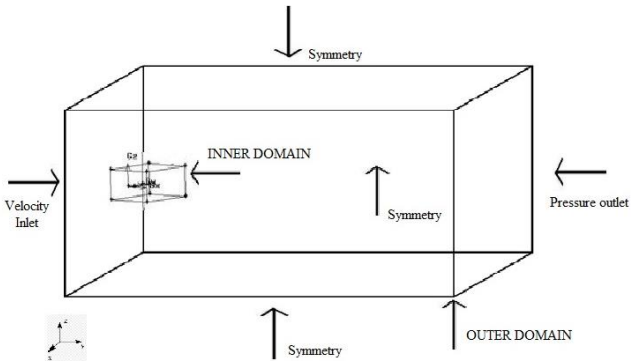

Fig. 5. Boundary conditions & Solution domain

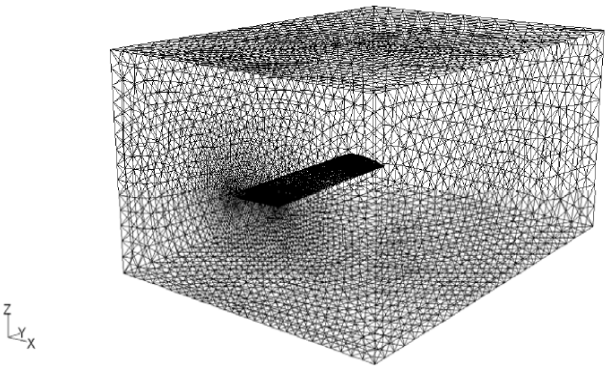

Fig. 6. Isometric view of inner domain

D. Modelling Solution

Pressure based solution is selected with node based gradient option and Spalart-Allmaras model is chosen for viscous condition and air is selected as the fluid with the specific properties (Density = 1.225 [kg/m3], Viscosity = 1.7894E-05 [kg/m-s]).

Spalart-Allmaras (SA) one-equation model is the most successful eddy viscosity models used today [12] and it has been designed for equilibrium flows where the turbulent time scales are much smaller than the mean flow time scales and react almost instantaneously to changes in the mean strain rate.

This assumption is very adequate for flows with no rapid changes in the flow field. However, the major flaw of one- and two- equation eddy viscosity models is that they do not account for history effects of the Reynolds stresses. Turbulence is produced by the mean strain rate in the flow. Under a non-equilibrium condition, the components of the strain rate tensor are constantly changing.

Thereby, various corrections to eddy viscosity models have been proposed to deal with this, such as the Spalart-Allmaras model with rotation and curvature correction (SARC) which suppresses turbulent production when the Reynolds stress tensor lags the mean strain rate tensor but does not actually model the physics of the lagging process [13, 14].

Some other equations were also added to an existing eddy viscosity model designed to relax the eddy viscosity towards an equilibrium value [15]. Lately, models have been studied which lag the RST instead of the eddy viscosity, called as the lagRST model developed [16], and was commenced for skin friction and separation predictions [15].

The Spalart-Allmaras (SA) turbulence model and the Menter k-ω shear-stress transport (SST) turbulence model have been widely-used and trusted models for Reynolds-averaged Navier-Stokes (RANS) computations of aerodynamic flows for well over a decade [17, 18].

Earlier, many CFD simulations in three dimensions have been investigated for high lift devices using these models, which include those of Mathias et al. [19] and Jones et al. [20] who studied a simple wing with half-span flap. Cao et al. [21] computed flow over a simplified Boeing 747 high lift configuration.

IV. Results And Discussions

Initially, the investigation of wing without span change having NACA4412 airfoil is performed. The results are presented as static pressure contour plots of upper and lower surfaces as seen in Fig. 7 and 8. It is clear from these figures that the leading edge has the highest pressure value in the wing. Also the chord-wise and span-wise pressure distribution is also clearly seen in the plot.

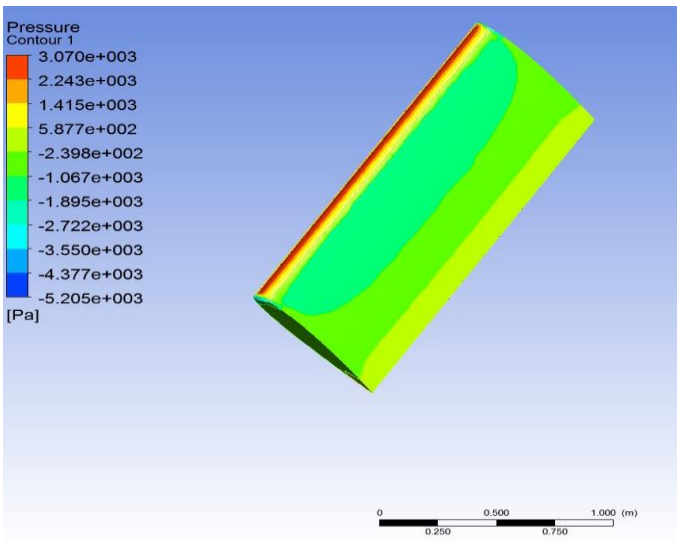

Fig. 7. Pressure distribution on upper surface of un-extended wing profile

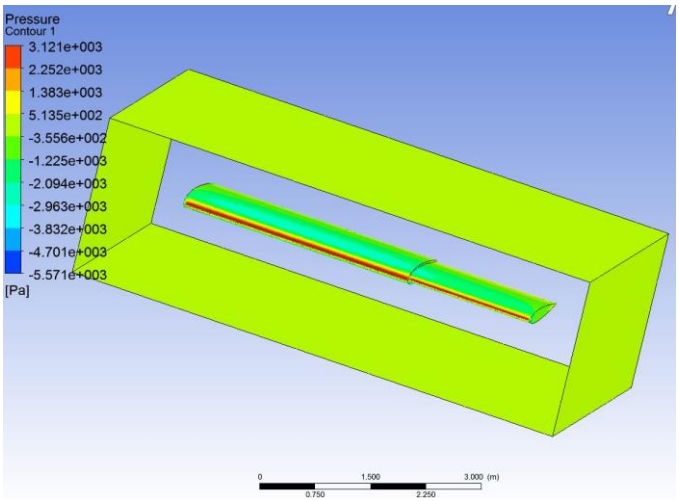

Fig. 8. Pressure distribution on upper surface extended wing profile

The second model is the wing profile with span extension. The results are presented as static pressure contour plots for upper and lower surface as seen in Fig. 9. The same pattern for pressure change is found in the morphed wing section (Fig. 10) with leading edge having higher pressure values.

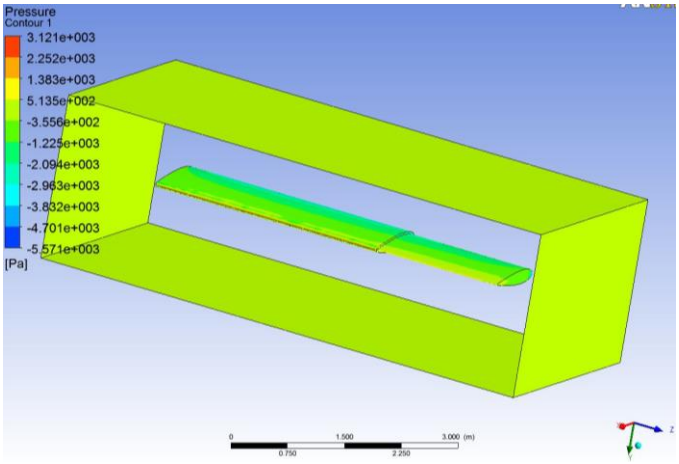

Fig. 9. Pressure distribution on lower surface of extended wing profile

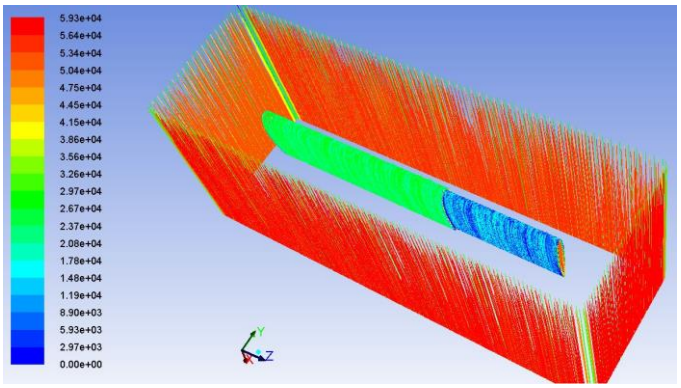

Fig. 10. Path lines distribution over the two wing sections.

The pressure variation is observed mostly in the extended wing section of the wing model. It is because during the extension, the flow in the wing tip coming from the lower surface disturbs the upper surface. The path lines are also presented to observe the flow pattern more accurately. It is seen that the extended wing section of the span adaptive model has denser path lines. It can attributed to the vortex generation phenomenon at the place where the wing section starts to extend and form a transition region for the flow.

V. Conclusions

This study investigates the computational design validation of an adaptive wing. An adaptive wing has been considered for augmenting the aerodynamic efficiency of an aircraft by varying the wing aspect ratio. The mesh morphing approach for shape optimization of grid-based numerical models has been presented. The application of this model showed a great potential of the quality meshing approach with the large time saving in the generation of good quality solution outcomes for modified geometry. Regarding the achieved results those small improvement seen are most likely due to the nature of the design variables and their limited number. The use of the mesh morphing methodology proves to be very helpful approach to minimize the computational cost of having to generate the mesh for every proposed configuration. In order to minimize the flaws in the results, it is recommended to consider more quality meshing using high fidelity simulation models. Future work will consider the possibility to employ the high fidelity simulation models for more accurate performance solutions. In this state we believe there will be a much higher improvement once the optimization will be achieved.

VI. References

[1] Beaverstock, C., Et Al. Optimising Mission Performance For A Morphing Mav. In Proceedings Of The Ankara International Aerospace Conference, Ankara, Turkey. 2013.

[2] Vocke, R.D., Et Al., Development And Testing Of A Span-Extending Morphing Wing. Journal Of Intelligent Material Systems And Structures, 2011: P. 1045389X11411121.

[3] Pecora, R., F. Amoroso, And L. Lecce, Effectiveness Of Wing Twist Morphing In Roll Control. Journal Of Aircraft, 2012. 49(6): P. 1666-1674.

[4] Prabhakar, N., Design And Dynamic Analysis Of A Variable-Sweep, Variable-Span Morphing UAV. 2014.

[5] Evans, C., Et Al., Development And Testing Of A Variable Camber Morphing Wing Mechanism. 2016.

[6] Bashir, M., Et Al., Outline For Mission-Based Morphing Evaluation With Smart Material Technology. International Journal Of Applied Engineering Research, 2016. 11(6): P. 4012-4016.

[7] Beaverstock, C.S., Et Al., Performance Comparison Between Optimised Camber And Span For A Morphing Wing. Aerospace, 2015. 2(3): P. 524-554.

[8] Ajaj, R., Et Al., Span Morphing Using The Gnatspar Wing. Aerospace Science And Technology, 2016. 53: P. 38-46.

[9] Ajaj, R., Et Al., The Zigzag Wingbox For A Span Morphing Wing. Aerospace Science And Technology, 2013. 28(1): P. 364-375.

[10] Woods, B.K. And M.I. Friswell, The Adaptive Aspect Ratio Morphing Wing: Design Concept And Low Fidelity Skin Optimization. Aerospace Science And Technology, 2015. 42: P. 209-217.

[11] Anderson, J.D., JR,"Introduction To Flight", 1989, Mc Graw-Hill International Editions, Aerospace Science Series.

[12] Rosen, A.M., Turbulence Modeling For Subsonic Separated Flows Over 2-D Airfoils And 3-D Wings. 2013.

[13] Spalart, P. And M. Shur, On The Sensitization Of Turbulence Models To Rotation And Curvature. Aerospace Science And Technology, 1997. 1(5): P. 297-302.

[14] Shur, M.L., Et Al., Turbulence Modeling In Rotating And Curved Channels: Assessing The Spalart-Shur Correction. AIAA Journal, 2000. 38(5): P. 784-792.

[15] Olsen, M.E., R.P. Lillard, And T.J. Coakley, The Lag Model Applied To High Speed Flows. AIAA Paper, 2005. 101: P. 2005.

[16] Lillard, R.P., Turbulence Modeling For Shock Wave/Turbulent Boundary Layer Interactions2011.

[17] Spalart, P.R. And S.R. Allmaras, A One Equation Turbulence Model For Aerodinamic Flows. AIAA Journal, 1992. 94.

[18] Rumsey, C.L. And P.R. Spalart, Turbulence Model Behavior In Low Reynolds Number Regions Of Aerodynamic Flowfields. AIAA Journal, 2009. 47(4): P. 982-993.

[19] Mathias, D.L., Et Al., Navier-Stokes Analysis Of The Flow About A Flap Edge. Journal Of Aircraft, 1998. 35(6): P. 833-838.

[20] Jones, K.M. And V. Hmpton, Application Of A Navier-Stokes Solver To The Analysis Of Multielement Airfoils And Wings Using Mulnzonal Grid Techniques. 1995.

[21] Cao, H.V., T. Su, And S.E. Rogers, Navier–Stokes Analysis Of A 747 High Lift Configuration. AIAA Paper, 1998. 98: P. 2623.